

Anisotropic Disorder in High Mobility 2D Heterostructures and its Correlation to Electron Transport

R.L. Willett, J.W.P. Hsu, D. Natelson, K.W. West, L.N. Pfeiffer
Bell Laboratories, Lucent Technologies, Murray Hill, NJ 07974

Surface morphology of high mobility heterostructures is examined and correlated with d.c. transport. *All* samples examined show evidence of lines in the $[1\bar{1}0]$ direction with roughness ranging from small amplitude features to severe anisotropic ridges. Transport in these samples is consistent with that in samples having artificially induced 1D charge modulations. The native surface properties reflect a prevalent, anisotropic disorder affecting 2D electron conduction. Importantly, the native lines are orthogonal to the stripes theoretically proposed to explain high Landau level transport anisotropies.

Correlated electron effects in 2D heterostructures can be observed because the disorder of these structures has been understood and subsequently controlled to facilitate low energy electronic interactions. The fractional quantum Hall effect (FQHE) [1] was observed in modulation doped heterostructures [2] as this specific device provides spatial separation of ionized impurities and the interacting 2D electron system (2DES). Molecular beam epitaxy (MBE) has produced extraordinarily pure systems [3] with electron mobilities exceeding 10^7 cm²/V-sec. Such structures exhibit phenomena ranging from composite fermion Fermi surface effects [4] at $\nu=1/2$, to transport anisotropies at high Landau levels [5,6], proposed to be electron stripe and bubble phases [7]. In the composite fermion system, density variations play a particularly significant role as disorder due to the association of charge and fictitious magnetic field [8]. Establishing sources of lateral charge variation within the high mobility interface is therefore important for understanding disorder influencing the correlated 2DES.

The surface of high mobility heterostructures provides an accessible plane to study possible density related disorder. Surface morphology can vary under different MBE growth conditions, and growth anisotropies can occur along certain crystallographic directions [9,11]. The length scales of these variations are large, on the order of microns, and so are imminently measureable. Key questions are then, do these large-scale imperfections occur in high mobility heterostructures, and do they influence the electronic properties of the 2D layer?

To answer this we have examined surface morphology using atomic force microscopy and studied transport of a series of high mobility heterostructures. In an extensive pool of high mobility wafers we observed a range of surface properties related to known crystal growth instabilities. Our principal finding is that *all* surfaces are observed to have some formation of ridges along the $[1\bar{1}0]$ direction. These lines exist within a range of large-scale topographic fluctuations that vary from nearly isotropic mounds to stark anisotropic ridges consistently along the $[1\bar{1}0]$ direction. Transport in samples with severe surface roughness is shown to be similar to that observed in het-

erostructures with artificially induced 1D charge density modulations [8,12]. In samples with the less severe native surface roughness, transport anisotropies can be identified in the lowest Landau level which are consistent with the surface morphology.

A focus of this study is the surface morphology of ultra-high mobility samples that demonstrate both extensive FQHE features and high Landau level transport anisotropies. These high quality samples show i) FQHE states manifest properties associated with the anisotropic growth, and ii) the native surface lines, which we associate with charge modulation as shown by transport, are oriented *orthogonally* to the stripes proposed in the theoretical models [13,7] of high Landau level anisotropies.

The MBE-produced wafers in this study were all grown on $[001]$ oriented substrates with a buffer layer of minimally $1\ \mu\text{m}$ thick GaAs or AlGaAs/GaAs superlattice. Transport properties and surface morphology were independent of whether heterostructures are single interfaces or quantum wells. The 2D layer resides less than 300 nm below the surface for all samples studied. The wafers focused upon here (and shown in Figures 1a-c) were produced under essentially the same conditions, indicating that the properties determining surface morphology are not well understood.

A large number of heterostructure wafers with mobilities greater than 8×10^6 cm²/V-sec were examined, and shown here are samples which are representative of the full range of surface morphologies. Light microscopy was also used to examine heterostructure surfaces; using phase contrast optics, most of the larger surface features can be detected readily at relatively low magnifications.

Surface morphology was examined using atomic force microscopy operating in tapping mode. Topographic images (Figure 1, right column) depict surface height variations. The change in cantilever oscillation amplitude, proportional to the derivative of topographic changes, is also shown (Fig. 1, left column). Transport was performed using standard lock-in techniques at low frequencies.

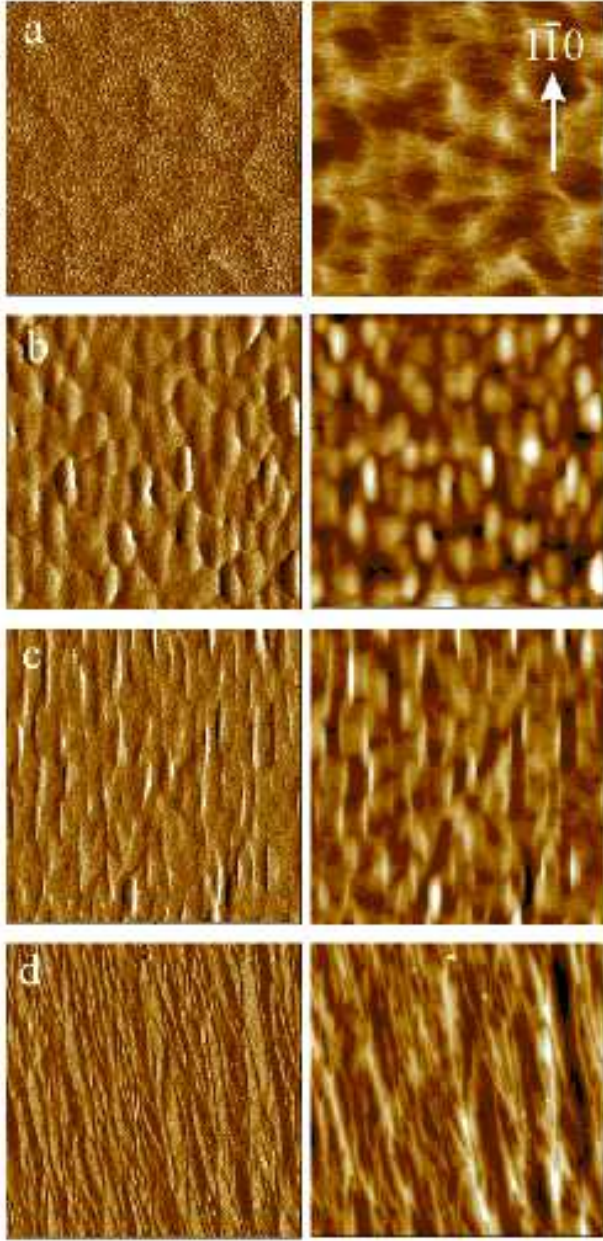


FIG. 1. Representative range of surface morphologies of high mobility heterostructures as measured with atomic force microscopy. Each field size is $20 \mu\text{m} \times 20 \mu\text{m}$. The images on the right are surface topography, and the images on the left show variations in cantilever amplitude which are proportional to the topography derivative. Sample mobilities and total vertical range for the topographic images (black to white) are (a) $16 \times 10^6 \text{ cm}^2/\text{V}\cdot\text{sec}$ and 40 \AA , (b) $27 \times 10^6 \text{ cm}^2/\text{V}\cdot\text{sec}$ and 100 \AA , (c) $23 \times 10^6 \text{ cm}^2/\text{V}\cdot\text{sec}$ and 100 \AA , (d) $8 \times 10^6 \text{ cm}^2/\text{V}\cdot\text{sec}$ and 300 \AA .

Figure 1 shows surface morphology for heterostructures ranging from smoothest (a) to roughest (d). All samples show features, lines, along the $[1\bar{1}0]$ direction. In the lowest overall amplitude surface topography, Figure 1(a), the dominant morphology is a coarsely isotropic

“orange peel” effect with a diameter of about $4 \mu\text{m}$ and height range of less than 40 \AA . Within these large features, fine lines corresponding to atomic scale terracing are observed aligned in the $[1\bar{1}0]$ direction. This predilection toward line formation in the $[1\bar{1}0]$ direction becomes more apparent as the overall surface roughness increases. In Figure 1(b) the orange peel texture has evolved to a surface with mounds clearly oriented in the $[1\bar{1}0]$ direction, and with vertical excursion of almost 100 \AA . Figure 1(c) shows another representative sample in the range of common surface morphologies. Severe ridges are present with about the same period as that shown in Figure 1(b) and with almost the same vertical excursion. It is important to note that wafers generally display morphology ranging from that shown in (a) to that shown in (c). The final AFM image (Figure 1d) shows an extreme case of surface roughness: this was induced by growing a particularly thick buffer layer of about $10 \mu\text{m}$, capped by a standard interface. The vertical excursion is large, up to 300 \AA , with line formation distinctly in the $[1\bar{1}0]$ direction. Note that ridges can traverse the full field of the scan.

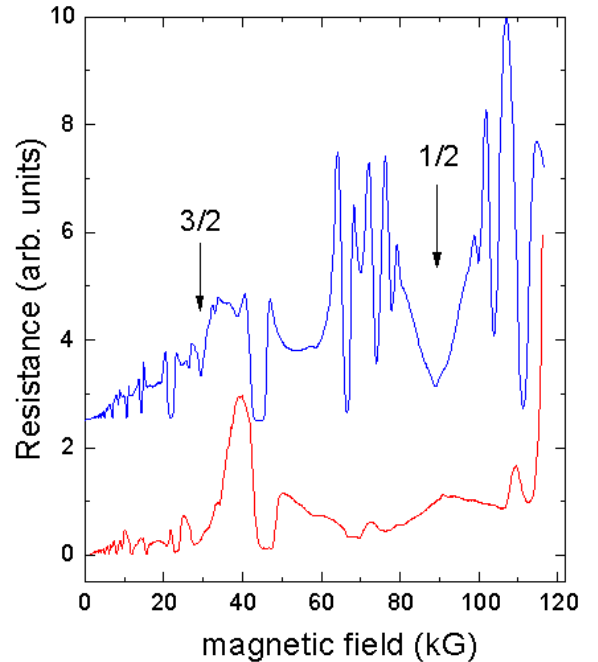


FIG. 2. Magnetotransport measured for the sample of Figure 1d. The red trace corresponds to current driven in the $[1\bar{1}0]$ direction and the blue trace is current driven in the $[110]$ direction. Temperature= 290 mK .

The common property of the above described range of morphologies is the formation of lines in the $[1\bar{1}0]$ direction. This effect is due to a previously recognized MBE growth instability [9] with fast growth rate along the direction of the As dangling bonds [10]. Extensive growth

or lowered temperatures during growth can accentuate this effect.

A second mechanism contributing to this formation of lines in the $[1\bar{1}0]$ direction is from the AlGaAs layering. A temperature and Al concentration dependent growth preference in the $[1\bar{1}0]$ direction has been documented [11]. It provides a smaller length scale ridge formation than the above described mechanism, and is at work in these samples due to the presence of GaAs/AlGaAs layering. Suppressing this contribution to ridge formation involves growth at the appropriate temperature and Al concentration; suppression of the previously noted growth instability is more difficult.

Transport results show that the surface morphology is associated with charge variation at the 2D electron layer. This precept is supported by the data of Figure 2: it shows typical transport data from the sample of Figure 1d having severe natural lines, with current driven across and along the $[1\bar{1}0]$ direction. The key features in this data are the large minimum in resistance at $1/2$ filling factor for current driven across $[1\bar{1}0]$ (across the native lines), accompanied by a peak at $1/2$ for current driven along $[1\bar{1}0]$. Note also that current driven across the native lines produces narrow FQHE states; conversely, current driven along the lines produces relatively widened FQHE states.

These effects are similar to those observed in transport in the lowest Landau level for a 1D charge density modulation artificially induced on a heterostructure: results from such a sample are shown in Figure 3. Artificial 1D charge density modulation is achieved by etching an array of lines into the surface of the heterostructure. The etch depth can be small, typically about 150 \AA , to induce transport consequences. The artificially modulated system shows a peak at $1/2$ for current driven along the imposed lines and a large minimum for current driven across the lines, just as seen in the sample of Figure 1(d) with native lines. In addition, the FQHE states show relative narrowing when current is driven across the modulation lines and broadening when driven along the modulation lines; again, this is similar to the effect observed for the respective transport directions in the native line sample of Figure 1(d). The central minimum and peak at $1/2$ for the two transport directions in the artificially modulated sample of Figure 3 show small features at and symmetrically about $1/2$. The lateral minima (peaks) correspond to geometric resonance of the charged carrier motion with the regular period of the modulation [14,15], and the central minimum (peak) at $1/2$ is due to “snake” states [16]. These occur as a consequence of large radius composite fermion cyclotron orbit motion along an effective B-field gradient centered about zero effective magnetic field, as expected to exist along the lines of a charge density gradient. Note the presence of such snake state transport at $1/2$ in the sample with strong native lines; the geometric resonances are absent due to the aperiodic nature of the

native charge modulation. Other features are common to the magnetotransport spectra of Figures 2 and 3; for example note the large peak between $\nu = 3/2$ and 1 in the red traces. The presence of these multiple specific features in both the native line sample and the artificially modulated sample clearly show empirically that the native surface lines in Figure 1d are indeed associated with charge modulations in the 2D electron layer.

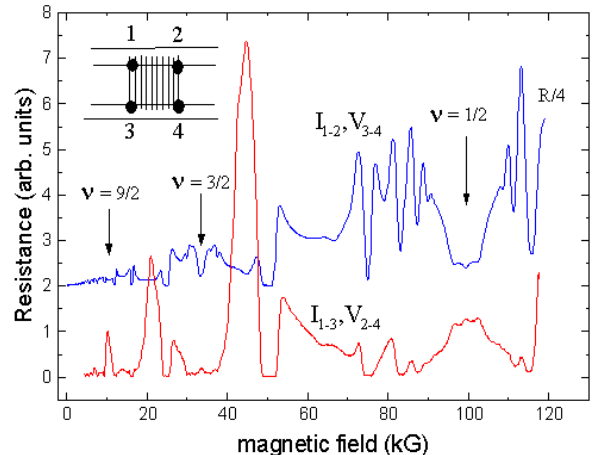


FIG. 3. Resistances as described by inset for 1D modulation etched into the heterostructure surface. The period of the modulation is $1.2 \mu\text{m}$ and the temperature is 290 mK .

Less coarse surface effects also produce transport consequences in the lowest Landau level. Shown in Figure 4(a) is the magnetotransport around $3/2$ for the sample pictured in Figure 1(c). The native modulations of this sample induce transport properties similar to those noted in the artificially charge modulated system: the FQHE states are wider in the orientation of current along the $[1\bar{1}0]$ direction (along the lines). This broadening of about $\delta B/B \sim 0.5\%$ reflects a spread in the density of $\delta n/n \sim 0.5\%$. This property was found in all of the large number of samples of similar surface morphologies that were examined. Additionally, current driven along the lines results in a less well developed minimum at $3/2$ and poorly formed high order fractions when compared to transport in the orthogonal direction. These specific effects are also observed in samples with less severe surface morphology. The sample shown in Figure 1b demonstrates similar broadening of the FQHE for current along the $[1\bar{1}0]$ direction, particularly at low temperatures ($< 100 \text{ mK}$). Samples with morphology approaching that of Figure 1a can likewise demonstrate these effects at very low temperatures.

A striking finding of our study is that samples with relatively severe surface morphology demonstrate beautifully the transport anisotropies in the high Landau levels that have recently been documented [5,6] and explained [7] using a new striped phase ground state. Figure 4(b)

shows transport in two directions from the sample of Figure 1(c), which has substantial native line formation in the $[1\bar{1}0]$ direction. Figure 4(b) shows the characteristic deep minimum at $9/2$ for current driven across the $[1\bar{1}0]$ direction (across the native lines) and also shows a peak at $9/2$ for current along the native lines. Empirically this is the same as the transport properties observed in the lowest Landau level for the artificially modulated 2DES. *Most importantly, the native lines observed in our morphology studies, which apparently act as charge lines as supported by the sample's lowest Landau level transport, are orthogonal to the theoretically proposed stripes used to explain the high Landau level transport.* The sample from Figure 1b, which has less severe but still significant anisotropy in the surface morphology shows similar high Landau level anisotropies.

In summary, surface morphology of high mobility heterostructures has been examined and found to show line formation in the $[1\bar{1}0]$ direction with varying degrees of severity over the full complement of wafers tested. These surface properties are correlated to transport results, with even mild surface roughness associated with distinct transport features. These transport features are like those seen specifically in samples with artificial 1D charge density modulations, suggesting similar transport mechanisms are at work in both systems. These pervasive native lines represent an important form of systematic, anisotropic disorder that is of particular significance in ultra-high mobility samples, as it is here that their consequences can be readily observed.

This finding of native density anisotropy in ultra-high mobility samples has particular pertinence in considering transport in high Landau levels, since the native lines are orthogonal to the direction of the stripes proposed theoretically to explain the transport anisotropy. It is tempting to consider that the same mechanism responsible for effects observed around $1/2$ in the artificial 1D charge modulated samples is at play at $9/2$ in the ultra-high mobility samples, with the 1D charge modulation provided by the native line formation. In spite of numerous empirical similarities, however, this is unlikely as Fermi surface formation would be required at the high Landau level half-filling. The native lines may have some influence in breaking the symmetry of the system, and so may induce orientation of the proposed ground state. This remains to be tested.

We show that surface morphology and its commensurate charge distribution have an impact on correlations in the 2DES. Further advancement in heterostructures designed to support electron correlation effects must overcome this systematic disorder.

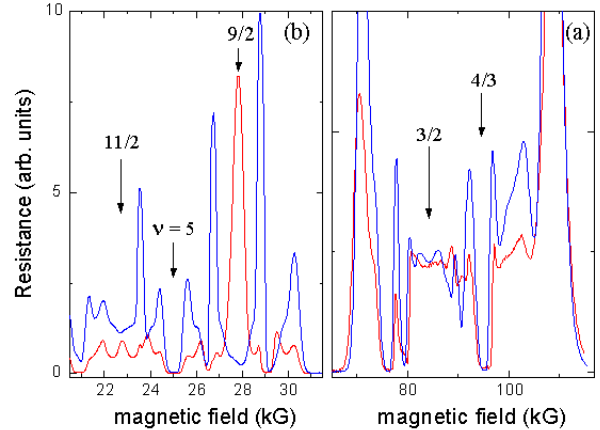


FIG. 4. Magnetotransport around filling factors $3/2$ (a) and $9/2$ (b) from the sample shown in Figure 1(c). The current is driven along $[110]$ (blue traces) or along $[1\bar{1}0]$ (red traces). The temperature is 110 mK. Substantially larger quantitative anisotropy at $9/2$ is observed at lower temperatures.

-
- [1] D.C. Tsui, H.L. Stormer, and A.C. Gossard, Phys. Rev. Lett. **48**, 1559 (1982).
 - [2] H.L. Stormer, R. Dingle, A.C. Gossard, W. Wiegmann, M.O. Sturge, Solid State Comm. **29**, 705 (1979).
 - [3] L. Pfeiffer, K.W. West, H.L. Stormer, K.W. Baldwin, Appl. Phys. Lett. **55**, 287 (1988).
 - [4] for overview see Composite Fermions, edited by O. Heinonen, (World Scientific, 1998).
 - [5] R.R. Du, D.C. Tsui, H.L. Stormer, L.N. Pfeiffer, K.W. West, Solid State Commun. **109**, 389 (1999).
 - [6] M.P. Lilly, K.B. Cooper, J.P. Eisenstein, L.N. Pfeiffer, K.W. West, Phys. Rev. Lett. **82**, 394 (1999).
 - [7] A.A. Koulakov, M.M. Fogler, B.I. Shklovskii, Phys. Rev. B **76**, 499 (1996) and R. Moessner, J. Chalker, Phys. Rev. B **54**, 5006 (1996).
 - [8] R.L. Willett, K.W. West, L.N. Pfeiffer, Phys. Rev. Lett. **78**, 4478 (1997).
 - [9] M.D. Johnson, C. Orme, A.W. Hunt, D. Graff, J. Suidjono, L.M. Sander, B.G. Orr, Phys. Rev. Lett. **72**, 116 (1994).
 - [10] R.M. Fleming, D.B. McWhan, A.C. Gossard, W. Wiegmann, and R.A. Logan, J. Appl. Phys. **51**, 357 (1980).
 - [11] F. Alexandre, L. Goldstein, G. Leroux, M. C. Joncour, H. Thibierge, E.V.K. Rao, J. Vac. Sci. Technol. B **3**, 950 (1985).
 - [12] J.H. Smet, K. von Klitzing, D. Weiss, W. Wegscheider, Phys. Rev. Lett. **80**, 4538 (1998).
 - [13] A.H. MacDonald, M.P.A. Fisher, Phys. Rev. B **61**, 5724 (2000).
 - [14] Felix von Oppen, Ady Stern, and Bertrand I. Halperin, Phys. Rev. Lett. **80**, 4494 (1998).
 - [15] R.L. Willett, K.W. West, L.N. Pfeiffer, Phys. Rev. Lett. **83**, 2624 (1999).
 - [16] J.E. Muller, Phys. Rev. Lett. **68**, 385 (1992).